ORIGINAL PAPER
Polish Journal of Microbiology
2024, Vol. 73, No 4, 475–489
https://doi.org/10.33073/pjm-2024-038

Comparative Genomic Analysis of an *Apiotrichum cacaoliposimilis* Strain Isolated from a Patient with Urinary Tract Infection

WEI WANG[1, 2], JINPING YI[1], JIAHUAN ZHAN[1, 2], DONG LUO[1], QIANG CHEN[1], SHENGMING YU[1, 2], LING XIE[1, 2] and KAISEN CHEN[1]*

[1] Department of Clinical Laboratory, the First Affiliated Hospital, Jiangxi Medical College, Nanchang University, Nanchang, China
[2] Department of Public Health, Jiangxi Medical College, Nanchang University, Nanchang, China

Submitted 18 June 2024, accepted 12 September 2024, published online 2 December 2024

Abstract

Opportunistic infections caused by fungi, particularly those occurring in immunocompromised patients, are considered challenging worldwide. Therefore, a comprehensive understanding of pathogenic fungi is necessary. The present study reports the isolation of a strain of *Apiotrichum cacaoliposimilis*, which is difficult to detect using conventional clinical assays, from the sterile urine samples of a patient with a urinary tract infection. Sanger sequencing of the internal transcribed spacer regions confirmed the genus of the microbe, while whole-genome sequencing yielded the initial genome assembly of *A. cacaoliposimilis*. A total of 7,161 predicted protein-coding genes were mapped using multiple databases, including Gene Ontology, Kyoto Encyclopedia of Genes and Genomes, non-redundant protein database, Pathogen-Host Interactions Database, and Comprehensive Antibiotic Resistance Database. The phenotypic data, biochemical reactions, and antimicrobial susceptibility analyses were conducted to reveal the metabolic properties, virulence, and drug resistance profile of the isolated *A. cacaoliposimilis*. The rank-sum test revealed the differences in the intergeneric distribution of the highly virulent genes *UgeB* and *Pem2*. In addition, other genes exhibited significant overlap in terms of virulence factors with the clinical isolate *Apiotrichum mycotoxinivorans* GMU1709. Fortunately, similar to most fungi belonging to the *Apiotrichum* genus, the isolate investigated in the present study was also sensitive to the drug voriconazole (MIC = 0.06 μg/ml). In summary, the phylogenetic placement, potential pathogenic genes, drug sensitivity patterns, and morphological characteristics of the isolated *A. cacaoliposimilis* were determined precisely in the present study.

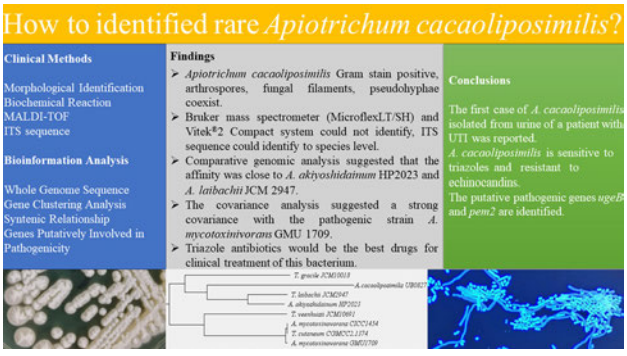

K e y w o r d s: drug susceptibility test, pathogenicity, phylogeny, species identification, whole-genome sequencing

Introduction

In 2015, the reclassification of class Tremellomycetes, which was established according to the molecular- rather than morphology- and physiology-based identification, led to the separation of the *Apiotrichum* genus from the *Trichosporon* genus (Liu et al. 2015a). *Apiotrichum cacaoliposimilis*, previously known as *Trichosporon cacaoliposimilis*, was first isolated in Japan, likely from a soil sample collected from a vegetable farm. While the exact ecological niche of *A. cacaoliposimilis* remains debatable to date (Gujjari et al. 2011), it reportedly thrives on fermentation media and produces cellular lipids similar to those in natural cocoa butter (Yang et al. 2024). *A. cacaoliposimilis* was initially considered an oleaginous yeast-like fungus, which is capable of synthesizing and accumulating lipids up to 70% of its dry weight and is, therefore explored for valuable commercial products such as biofuels and cocoa butter equivalent (CBE) (Ghazani and Marangoni 2022).

* Corresponding author: K. Chen, Department of Clinical Laboratory, the First Affiliated Hospital, Jiangxi Medical College, Nanchang University, Nanchang, China; **e-mail: chenks100@126.com**

The pathogenic potential of *A. cacaoliposimilis* is, however, not reported extensively in the clinical literature, which contains just one report on the isolation of *A. cacaoliposimilis* from a nail sample from a patient with onychomycosis (Noguchi et al. 2020). The knowledge regarding the diagnosis and treatment of *A. cacaoliposimilis* is limited to this single case report, and the complete genome of *A. cacaoliposimilis* is currently unavailable. *Trichosporon* is a genus related closely to *A. cacaoliposimilis*, and *Trichosporon* spp. have, to the best of the author's knowledge, a pivotal role in different clinical infections. *Trichosporon* spp. resides occasionally on the skin surface and within the gastrointestinal environment in humans and comprises a diverse range of opportunistic pathogens that cause infections (Colombo et al. 2011; Noguchi et al. 2020) observed frequently in patients admitted to the intensive care units, particularly in patients with hematological malignancies or neutropenia and those undergoing broad-spectrum antibiotic therapy or invasive surgery (Francisco et al. 2019). The precise identification of the etiological agents at the taxonomic level is crucial, considering the variable antifungal drug susceptibilities of different *Trichosporon* spp. (Guo et al. 2019). The commercially available systems, such as API® 20 C AUX and Vitek® 2 Compact YST manufactured by bioMérieux (France), often yield uncertain results when rare species are involved (Guo et al. 2011). Moreover, the mass spectrometry-based libraries are enriched more with the commonly identified clinical pathogens, and their utility in detecting rare fungi is limited (Francisco et al. 2023). The internal transcribed spacer (ITS) sequencing facilitates a precise identification of yeast species (Langsiri et al. 2023), although it has not been adopted widely in clinical settings.

The existing literature on *A. cacaoliposimilis* is, to the best of the author's knowledge, limited to species-level classification based on ITS and D1/D2 sequencing, biochemical responses, and drug susceptibility tests (Gujjari et al. 2011; Noguchi et al. 2020). The NCBI database contains 27 species within the *Apiotrichum* genus, including *A. cacaoliposimilis* (NCBI:txid105983). Among these species, at least six are reportedly associated with opportunistic infections (Taverna et al. 2014; Lara et al. 2019; Peng et al. 2019; Premamalini et al. 2019). However, previous studies lack a genomic analysis of *A. cacaoliposimilis*. Therefore, the present study was conducted to provide a reference for identifying the clinically rare pathogenic fungus *A. cacaoliposimilis*. Since the present report is a pioneer genome-wide report on this fungus, the meaningful annotation of the virulence genes of this fungus published in this report will serve as a basis for future research on the pathogenic mechanisms of this fungus. Further, the clinical protocols for treating this fungal infection will be elaborated based on the drug sensitivity test (DST).

Experimental

Materials and Methods

Patient and specimens. A male patient aged 70 years presented to the emergency department of our hospital with the complaint of left lumbar discomfort and pyrexia (38°C). The patient also stated experiencing right upper abdominal pain, difficulty in urination, weak urine stream, and an increase in urinary frequency, urgency, and dysuria. A urological ultrasound revealed stones in the upper left ureter and left hydronephrosis. Physical examination elicited positive percussion pain above the left kidney. The patient was, therefore, provided with a primary diagnosis of left ureteral calculus accompanied by hydronephrosis and infection and a secondary diagnosis of UTI. Subsequently, the patient was admitted to the outpatient clinic of the hospital, where the laboratory tests revealed elevated white blood cell count (WBC) (17.58×10^9/l), high neutrophil percentage (95.4%), and increased levels of C-reactive protein (CRP) (173.85 mg/l), procalcitonin (PCT) (2.66 ng/ml), and creatinine (CR) (118.9 μmol/l). The other clinical findings were as follows: urinary leukocyte esterase, 1+/70 cells/μl; urinary erythrocytes, 289/μl; urinary leukocytes, 149/μl. In the period of hospitalization, the patient exhibited persisting pyrexia despite receiving the standard antibiotic therapy. Therefore, the mid-stream urine specimen was promptly sent to the clinical microbiology laboratory for inoculation and culture. After 48 hours of culture, no bacterial colony was detected, although fungal growth was noted. However, the mass spectrometry of the typical colonies with low confidence, smear microscopy, and biochemical analyses indicated the presence of an uncommon fungus, which was labeled UB0827 and analyzed further for identification. The subsequent susceptibility tests indicated sensitivity to antifungal medications. After that, the patient was administered voriconazole at an initial dose of 6 mg/kg every 12 h for a day, followed by a maintenance dose of the drug at 3 mg/kg every 12 h for three days. The treatment normalized the patient's temperature on the third day of the antifungal treatment, after which the patient was discharged from the hospital.

Materials. Sabouraud agar with ATB® FUNGUS 3 (bioMérieux, France) was used in fungal drug sensitivity testing. Vitek® 2 Compact (bioMérieux, France), equipped with a YST identification card, was used for fungal identification. A MALDI-TOF mass spectrometer (Bruker Daltonics GmbH & Co., Germany) was employed to validate the identification. Gram staining, lactophenol cotton blue staining, fluorescence staining, and hexamine silver staining were performed using the respective reagents from Zhuhai Baso Biotechnology Company (China).

Morphological identification. Microbial culture was performed using the Sabouraud agar medium at 35°C for 72 h. The isolates were then analyzed using Gram staining, lactophenol cotton blue staining, fluorescent staining, and hexamethylamine silver staining. The stained samples were photographed under a microscope for further analysis.

Biochemical reactions and mass spectrometry. Three to five colonies developed on the Sabouraud agar medium culture were isolated and resuspended in a 0.45% solution of sterile saline, followed by adjusting the suspension culture density to the McFarland concentration of 1.8–2.2. The suspension culture was then transferred to a tube containing the YST identification card, and incubation was performed in the Vitek® 2 Compact system for 24 h. A total of three independent replicates were used for the test.

The fungal samples were placed on the designated regions on a VITEK® MS-DS target slide and spread uniformly using a 1 µl inoculation loop according to the manufacturer's instructions. Subsequently, 0.5 µl of the VITEK® MS-FA reagent was placed on each designated spot, and after 1–3 min, 1 µl of the VITEK® MS-CHCA matrix solution was added. After drying, the samples were processed using the VITEK® MS instrument.

Drug susceptibility testing. ATB® FUNGUS 3 was utilized to select colonies from the Sabouraud agar medium, following the manufacturer's instructions. The selected colonies were then suspended in 0.85% NaCl solution, and the McFarland turbidity was adjusted to 2.0 using the McFarland turbidimeter. Next, 20 µl of the resulting culture solution was transferred to ATB® FUNGUS 3. After adding the solution to the sealed wells containing the antifungal drug, it was incubated at 35.8°C for 48 h. Fungal growth in each well was compared to that in the blank control well to determine the minimum inhibitory concentration.

ITS and genome sequencing. The fungal lysates for ITS sequencing were obtained using the TaKaRa lysis buffer for the microorganism provided in the PCR kit (Code No. 9164; Takara Bio Inc., Japan) according to the manufacturer's instructions. First, a single colony was lysed in a microtube by adding 50 µl of the lysis buffer. Next, the resulting lysate was vortexed thoroughly followed by denaturation at 80°C for 15 min and centrifuged at 1,000 × *g* to precipitate cell debris. The resulting clear supernatant was subjected to a polymerase chain reaction (PCR) to amplify the DNA content for further analysis. The PCR reaction mixture contained 1–5 µl of the lysate supernatant, 25 µl of Premix Taq, 1 µl of the Forward Primer (10 pmol/µl), and 1 µl of the Reverse Primer (10 pmol/µl), and was supplemented with sterile nuclease-free water to reach a total volume of 50 µl. The primers used in the PCR were ITS1 (5'-TCCGTAGGTGAACCTGCGG-3') and ITS4 (5'-TCCTCCGCTTATTGATATGC-3'), which were designed by Gujjari et al. (2011). The PCR products were confirmed using 1% agarose gel electrophoresis, and the target sequences were recovered using the TIANGEN gel recovery kit (TIANGEN Biotech(Beijing)Co., Ltd., China). The recovered sequences were analyzed through Sanger sequencing (Beijing Prime Biotechnology Co., China).

Genomic DNA was extracted from a frozen colony using the cetyltrimethylammonium bromide protocol (Kim et al. 2010). The DNA samples were then fragmented randomly using a Covaris ultrasonic crusher (Covaris, LLC., USA). Library preparation involved end repair, addition of the A-tail and sequencing junction, PCR, fragment screening, and purification. Multiple libraries with the same effective concentration and the desired downstream data volume were pooled and subjected to double-end sequencing (Illumina, Inc., USA). The quality control of the sequencing data involved the removal of the reads with > 40% low-quality bases (quality ≤ 20), ≥ 10% unknown bases, and 15 bp overlap with adapter sequences. The sequencing data were then assembled using SOAP denovo (v2.04) (Luo et al. 2012) with GapCloser (v1.12). Sequences < 500 bp in length were filtered out, and the remaining sequences were subjected to a statistical analysis and gene prediction. Genomic completeness was assessed based on the BUSCO score (Simão et al. 2015), and the ratio of the Illumina reads was mapped back to the genome.

Phylogenetic analysis. The ITS and whole genome sequences of various species (Table SI) were downloaded from the NCBI genome database. The ITS sequences obtained from Sanger sequencing were aligned with those downloaded from the NCBI genome database using Muscle5 (Edgar 2022). Phylogenetic trees were then constructed using the maximum likelihood method using IQ-tree (v2.0) (Minh et al. 2020).

Mugsy (v1.2.3) (Angiuoli and Salzberg 2011) was employed to identify and extract the homologous regions between the assembled genome and reference genomes from the selected species, which were annotated in the MAF format. These files were subsequently converted to the FASTA format and aligned using MAF to FASTA (v1.0.1) in Galaxy (Galaxy Community 2022). The homologous regions with high-quality alignments were extracted using trimAl (v1.4.1) with default parameters (Capella-Gutiérrez et al. 2009), and the gaps were removed using Seqkit (v2.6.1) (Shen et al. 2016; 2024). The resulting sequences were compared with default parameters using MAFFT (v7.520) (Rozewicki et al. 2019). Finally, a maximum likelihood tree was constructed using RAxML (v8.2.13) (Stamatakis 2014). The bootstrap confidence intervals were calculated based on 1000 replicates.

Gene prediction and functional annotation. RepeatMasker software (v open-4.0.5; http://www.

repeatmasker.org) was employed to identify and mask the scattered repeat sequences. Tandem repeats in the DNA sequences were searched using Tandem Repeats Finder (v4.07b) (Benson 1999). The transfer RNAs and ribosomal RNAs were predicted using tRNAscan-SE (v1.3.1) (Lowe and Eddy 1997) and RNAmmer (v1.2) (Lagesen et al. 2007), respectively. Comparative annotation was performed using Rfam (Kalvari et al. 2021) to identify the bacterial small RNAs, small nuclear RNAs, and micro RNAs. CMsearch (v1.1rc4) was used with default parameters to confirm the bacterial small RNA annotations.

The coding genes in the newly sequenced genome were predicted using Funannotate (v1.8.1) (Palmer and Stajich 2020). The protein sequences encoded by these predicted genes were compared against those in the functional databases, such as GO, KEGG, NR, and CAZy using Diamond (v2.0.11.149) (Buchfink et al. 2021) and an e-value threshold of ≤ 1e-5. The sequences with ≥ 40% identity and ≥ 40% coverage were then selected and annotated. The signal peptides and transmembrane structures were identified using SignalP (v4.1) (Petersen et al. 2011) and TMHMM (v2.0c) (Sonnhammer et al. 1998; Krogh et al. 2001), respectively, which facilitated the prediction of the secreted proteins. AntiSMASH (v2.0.2) (Blin et al. 2013) was utilized to predict the secondary metabolic gene clusters in the genome.

Orthologous gene families and synteny analysis. The genome sequences of *Apiotrichum*, *Trichosporon*, *Cutaneotrichosporon*, and *Vanrija* were obtained from the NCBI genome database. The downloaded dataset included the reference sequences of 81 species (Table SI). Since gene and protein annotations were lacking for most of these species, gene prediction was performed using Funannotate (v1.8.1). Gene clustering analysis was then performed using OrthoMCL and OrthoVenn3 (https://orthovenn3.bioinfotoolkits.net) with default parameters. Synteny analysis was also conducted using MCScanX in TBtools (Chen et al. 2023). Inter-species comparisons were conducted by selecting the representative species from closely related genera, including *Apiotrichum* (*A. porosum* DSM 27194, *A. brassicae* JCM 1599, *A. mycotoxinovorans* GMU1709, and *A. gracile* JCM 10018), *Trichosporon*, and *Cutaneotrichosporon* (*T. asahii* CBS 2479 and *C. oleaginosum* IBC 0246). Intra-node comparisons were conducted by focusing on *Apiotrichum akiyoshidainum* HP2023 and *Apiotrichum laibachii* JCM 2947. The primary objective of this comparative genomic analysis was to elucidate the intricate evolutionary relationships among these genomes.

Identification of the virulence and resistance genes. Fungal virulence and resistance genes were identified, and the pathogenicity-related intraspecies and intergeneric genetic differences were determined using BLASTp in Diamond (v2.0.11.149) with the following parameters: e-value 1e-5; query coverage 40; identity 40; ultra-sensitive. Protein sequences were mapped to several databases, including the Mycology Antifungal Resistance Database (Nash et al. 2018), Pathogen-Host Interactions database (PHI-base) (Urban et al. 2022), Comprehensive Antibiotic Resistance Database (Alcock et al. 2023), and the database of fungal virulence factors. Wilcox test was performed using SPSS® 28.0 software (IBM® SPSS® Statistics for Windows, version 28.0, IBM Corp., USA) to determine the inter-group differences. The results were visualized using TBtools.

Results

Morphological identification. On the third day of incubation at 35°C for strain UB0827, the largest creamy white colonies, each 35 mm in diameter, with a fuzzy texture and irregular edges, were observed. The surface folds of these colonies had a ridged center on Sabouraud's medium (Fig. 1A). After Gram staining, dark purple subglobular, ovoid, oval cells approximately 3–6 μm in diameter and the formation of potential arthrospores from violet mycelium shedding was noted at 1000× magnification (Fig. 1B). Lactophenol Cotton Blue staining highlighted the blue-stained oval, short rod-like structures and translucent structures with granular-like organelles inside spores (Fig. 1C). The hexamethylene-silver staining revealed mycelium in a paler greenish color, highlighting the junctions where the distinct potential arthrospores were connected (Fig. 1D). When observed under a fluorescence microscope, the fungal hyphae and budding spores exhibited a distinctive feature of emitting a vibrant blue fluorescence under UV light (Fig. 1E).

Species identification. The results of the biochemical tests conducted using Vitek® 2 Compact are presented in Table I. The identified potential suspects were *Cryptococcus laurentii* (*Papiliotrema laurentii*) and *T. asahii*. A comparison of the biochemical characteristics of *A. mycotoxinivorans* GMU 1709 and *A. cacaoliposimilis* ATCC® 20505™ (Gujjari et al. 2011; Peng et al. 2019) revealed that strain UB0827 exhibited weak responses in saccharification, nitrate, and citrate assimilation reactions. Moreover, the mass spectrometry analyses conducted using the MALDI-TOF technology did not support biochemical identification, and the confidence level was relatively low.

A comparison of the sequenced ITS regions using BLAST yielded several results with > 99% identity and ≤ 3 gaps. The neighbor-joining tree (Fig. S1a) for the top 10 results, constructed using the Distance tree function of Web results, revealed a close relationship between the species isolated in the present study and *A. cacaoli-*

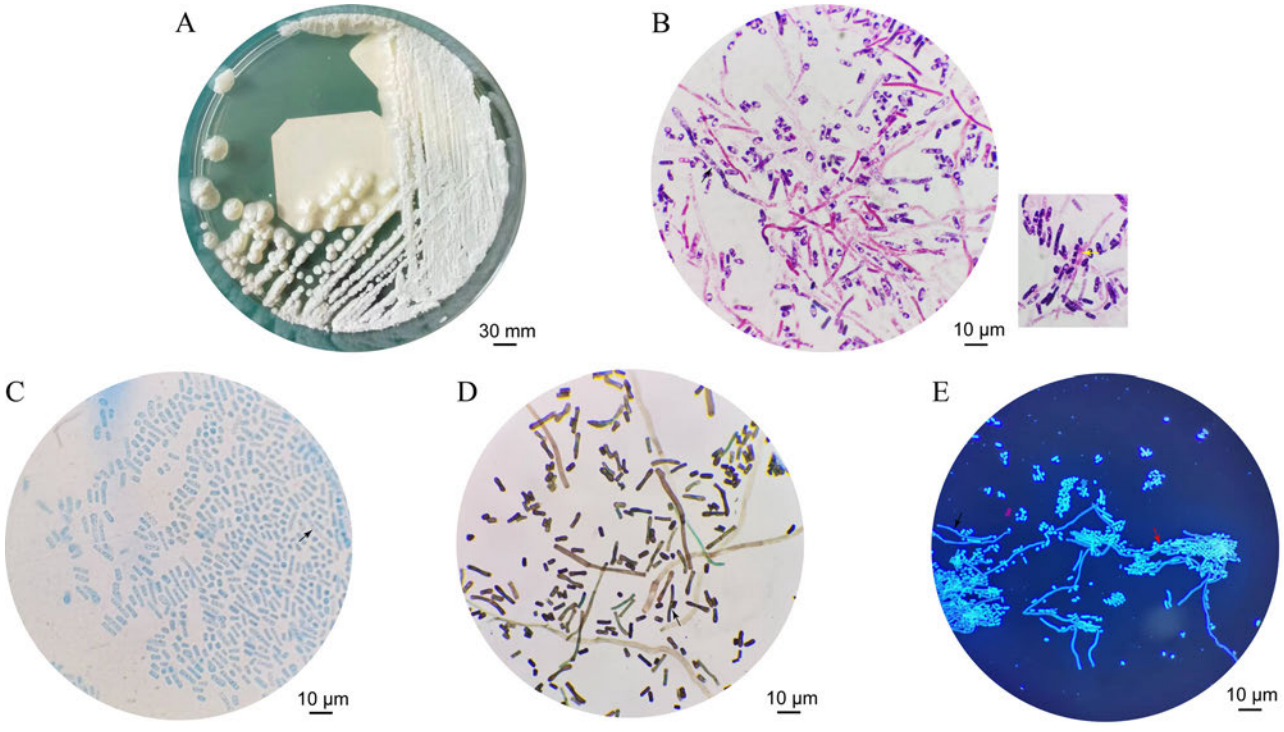

Fig. 1. Morphology of the UB0827 strain: A) image after incubation on Sabouraud's medium for 3 days; B) Gram staining under the microscope (1000× magnification); C) lactophenol cotton blue staining under the microscope (1000× magnification); D) hexamethylamine silver staining under the microscope (1000× magnification); E) fluorescent staining under the microscope (1000 magnification). Black arrows indicate the fungal filaments. Yellow arrows indicate the potential arthrospores. Red arrows indicate the budding spores.

posimilis. The maximum likelihood tree (Fig. S1b) constructed based on the ITS sequences revealed that the isolated strain UB0827 was closely related to *A. cacaoliposimilis* and *A. akiyoshidainum*. Even after 5,000 repetitions of random sampling, the best Bootstrap value could not be obtained because UB0827 was situated at the wrong branch relative to *A. akiyoshidainum*.

Antifungal susceptibility testing. The antifungal susceptibility testing conducted using ATB® FUNGUS 3 revealed the following results in terms of the minimum inhibitory concentrations of multiple antifungal drugs: amphotericin B, 0.5 µg/ml; 5-fluorocytosine, 2 µg/ml; triazole antibiotic fluconazole, 2 µg/ml; itraconazole, 0.12 µg/ml; voriconazole, 0.06 µg/ml; posaconazole, 6 µg/ml; echinocandin antibiotic, 8 µg/ml (Table II).

Whole-Genome analysis. Genomic data of approximately 2.56 Gb in quantity were generated through Illumina sequencing. The 15-mer analysis was then conducted to estimate the actual and fitted genome sizes, which were 25.6 Mb and 26.27 Mb, respectively, using a *k*-mer depth of 33.31 × (average sequence depth 69×). The scaffold N50 was approximately 406.6 Kb. The average GC content was approximately 60.83%, and 88.2% of the complete BUSCO genes in the genome of *A. cacaoliposimilis* UB0827 belonged to the expected class Tremellomycetes (Fig. S2).

Using RepeatMasker and Tandem Repeats Finder, a total of 2,525,374 bp of repetitive sequences were detected in the evaluated genome, including 681,841 bp of long terminal repeats, 251,865 bp of long scattered repeats, 253,304 bp of short, scattered repeats, 271,919 bp of DNA repeats, 124,837 bp of minisatellite DNA, and 25,926 bp of microsatellite DNA. Homology-based and *ab initio* prediction analyses revealed 7,161 protein-coding genes in the evaluated genome, with an average length of approximately 1,702.19 bp. Among these genes, 6,734 genes encoded messenger RNAs and 427 genes encoded transfer RNAs. The average number of exons in these genes was approximately 4.35, with an average length of 312.4 bp. The average length of the proteins encoded by these genes was approximately 467.34 amino acids. Eleven small nuclear RNAs could be aligned, although no validated ribosomal RNAs were predicted. Annotation with the Gene Ontology database revealed 4,549 gene classes, including 8,692 in the category of biological processes, 5,663 in the category of cellular components, and 5,422 in the category of molecular functions. The weight of each of these classes is presented in Fig. 2. Further, 3,270 genes were annotated in the Kyoto Encyclopedia of Genes and Genomes, and most of these genes were related to infectious diseases. In addition, these genes were involved in various pathways, most related to carbohydrate and amino acid metabolism (Fig. S3a).

The genome-wide phylogenetic tree (Fig. 3) confirmed that the isolated *A. cacaoliposimilis* belonged

Table I
The following are the different/important biochemical reactions between strains *Apiotrichum cacaoliposimilis* UB0827, ATCC® 20505™ and *Apiotrichum mycotoxinovorans* GMU1709.

Biochemical reaction	Strain		
	UB0827	ATCC® 20505™	GMU1709
L-lysine-arylamidase	–	+	–
Erythritol assimilation	–	–	–
Glycerol assimilation	–	+	+
β-*N*-Acetyl-glucosaminidase	–	+	+
Arbutin assimilation	–	+	–
Methyl-α-D-glucopyranoside assimilation	–	+	–
D-Raffinose assimilation	–	–	+
PNP-*N*-acetyl-β-D-galactosaminidase 1	–	–	+
D-Melibiose assimilation	–	D	+
D-Melezitose assimilation	–	+	–
L-Sorbose assimilation	–	+	–
Xylitol assimilation	–	+	–
D-Sorbitol assimilation	–	/	+
Urease	+	+	+
D-Trehalose assimilation	+	+	+
Nitrate assimilation	–	+	+
D-Galacturonate assimilation	+	–	+
Esculin hydrolysis	–	/	+
DL-Lactate assimilation	+	–	+
Citrate (sodium) assimilation	–	D/W	+

Assimilation reactions: D-galactose (+), D-glucose (+), lactose (+), D-cellobiose (+), D-maltose (+), saccharose/sucrose (+), L-arabinose (+), D-xylose (+), 2-keto-D-gluconate (+), D-gluconate (+)
+ – positive, – – negative, D – delayed positive, W – weak positive

Table II
Antifungal susceptibility of *Apiotrichum cacaoliposimilis* UB0827.

Antifungal susceptibility (MICs, μg/ml)								
5FC	AMB	FLU	POS	VOR	ITZ	ANID	MICA	CASP
2	0.5	2	0.06	0.06	0.12	8	8	8

5FC – 5-fluorocytosine, AMB – amphotericin B, FLU – fluconazole, POS – posaconazole, VOR – voriconazole, ITZ – itraconazole, ANID – anidulafungin, MICA – micafungin, CASP – caspofungin, MICs – Minimum Inhibitory Concentrations

to the *Apiotrichum* genus, consistent with the ITS sequence alignment results. The tree, with a Bootstrap value of 100, obtained from 1,000 random replicates, placed the isolated strain at the same node as that of *A. akiyoshidainum* HP2023 and *A. laibachii* JCM 2947. The branch lengths distinguished the isolated strain from *A. akiyoshidainum* HP2023, indicating that this fungus belonged to the *A. cacaoliposimilis* species. Moreover, the evolutionary relationship noted between *A. akiyoshidainum* HP2023 and *T. cutaneum* ACCC 20271 was consistent with the report of Peng et al. (2022). Accordingly, a highly reliable evolutionary relationship of the isolated fungus was established, named *A. cacaoliposimilis* UB0827. However, since this is the first strain to be sequenced without intra-specific whole-genome sequence comparisons, further confirmation of this phylogenetic relationship is necessary.

Gene clustering analysis. Markov clustering analysis identified 454,970 protein sets from the 81 strains (Table SI) belonging to the four genera of *Trichosporonaceae*. Among these sets, 98.2% (446,773) of the protein sets were clustered into 15,425 orthologous groups, with 319 orthogroups specific to certain species. The evolutionary positions among 81 species in

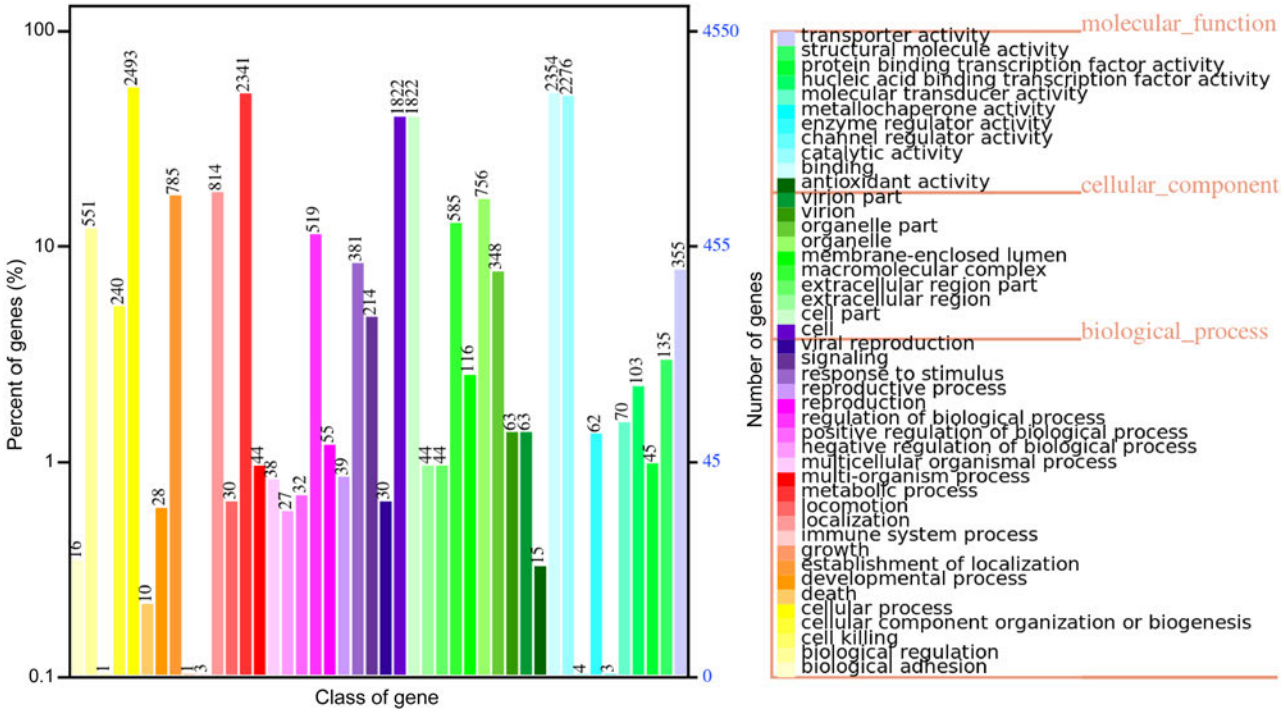

Fig. 2. The legend on the right side of the figure lists the functional classifications of the Gene Ontology (GO) annotations for the corresponding samples under the three categories of GO ontology classifications. The left side of the figure depicts the distribution of a number of GO functional analyses on the annotations. The horizontal axis represents the number of genes, displayed in different colors corresponding to the different types mentioned in the legend on the right. The vertical axis presents the GO functional classification.

the genome-wide phylogenetic tree were validated by constructing the maximum likelihood tree based on the homologous gene families (Fig. S4). The Venn diagram (Fig. 4A) analysis and comparison of *A. cacaoliposimilis* UB0827 with the four genera of *Trichosporonacea* revealed that the *A. cacaoliposimilis* strain UB0827 shared the highest number of orthogroups with the *Apiotrichum* genus (*Apiotrichum*: 5,161 > *Cutaneotrichosporon*: 4,822 > *Trichosporon*: 4,007 > *Vanrija*: 3,784). This finding is supported by the non-redundant protein database annotations, according to which the homologous proteins of *A. porosum* are more numerous than any other species (Fig. S3b). Further, Fig. 4B presents the comparison of the four branches (*A. cacaoliposimilis* UB0827, *A. akiyoshidainum* HP2023, *A. gracile* JCM10018, and *A. laibachii* JCM2947) to the orthogroups, illustrating the intersections of 4,941, 4,529, and 5,302, respectively. These results supported the observed genome-wide phylogenetic relationships.

Syntenic relationship. Genomic synteny block analysis discerned the evolutionary relationships among the different strains, revealing synteny among *A. cacaoliposimilis* UB0827, *A. gracile* JCM10018, and *A. laibachii* JCM2947 (Fig. 5). Notably, *A. cacaoliposimilis* UB0827 exhibited a considerable degree of synteny with *A. mycotoxinivorans* GMU 1709. However, this synteny was not as extensive as that demonstrated with *A. gracile* JCM10018, affirming their evolutionary linkage. In contrast, *A. akiyoshidainum* HP2023 exhibited lesser synteny. A separate comparison of *A. cacaoliposimilis* UB0827, *A. gracile* JCM10018, and *A. laibachii* JCM2947 revealed 2154, 1557, and 3683 synteny blocks, respectively (Fig. S5), demonstrating the evolutionary connections among these four. The observed differences could be attributed mainly to the quality of genome assembly. These findings corroborated the evolutionary affiliation of *A. cacaoliposimilis* UB0827 within the *Trichosporonaceae* family.

Genes putatively involved in pathogenicity. PHI-base is a gene-centric database of paramount significance, which curates the experimentally validated virulence, pathogenicity, and effector genes sourced from diverse pathogens. Each gene in this database has been assigned a distinctive PHI-base accession number, facilitating a streamlined identification and retrieval process. This comprehensive database has an expansive array of included pathogens, encompassing interactions with a broad spectrum of hosts, due to which it assumes a pivotal role in unearthing the pathogenicity-linked genes from emergent opportunistic pathogens (Urban et al. 2022). The identification of such genes would facilitate the identification of potential targets for interventions to combat the harmful influence of these pathogens. The current iteration of PHI-base version 4.16 boasts an impressive compendium documenting an astounding 9,666 genes and 21,676 interactions linked

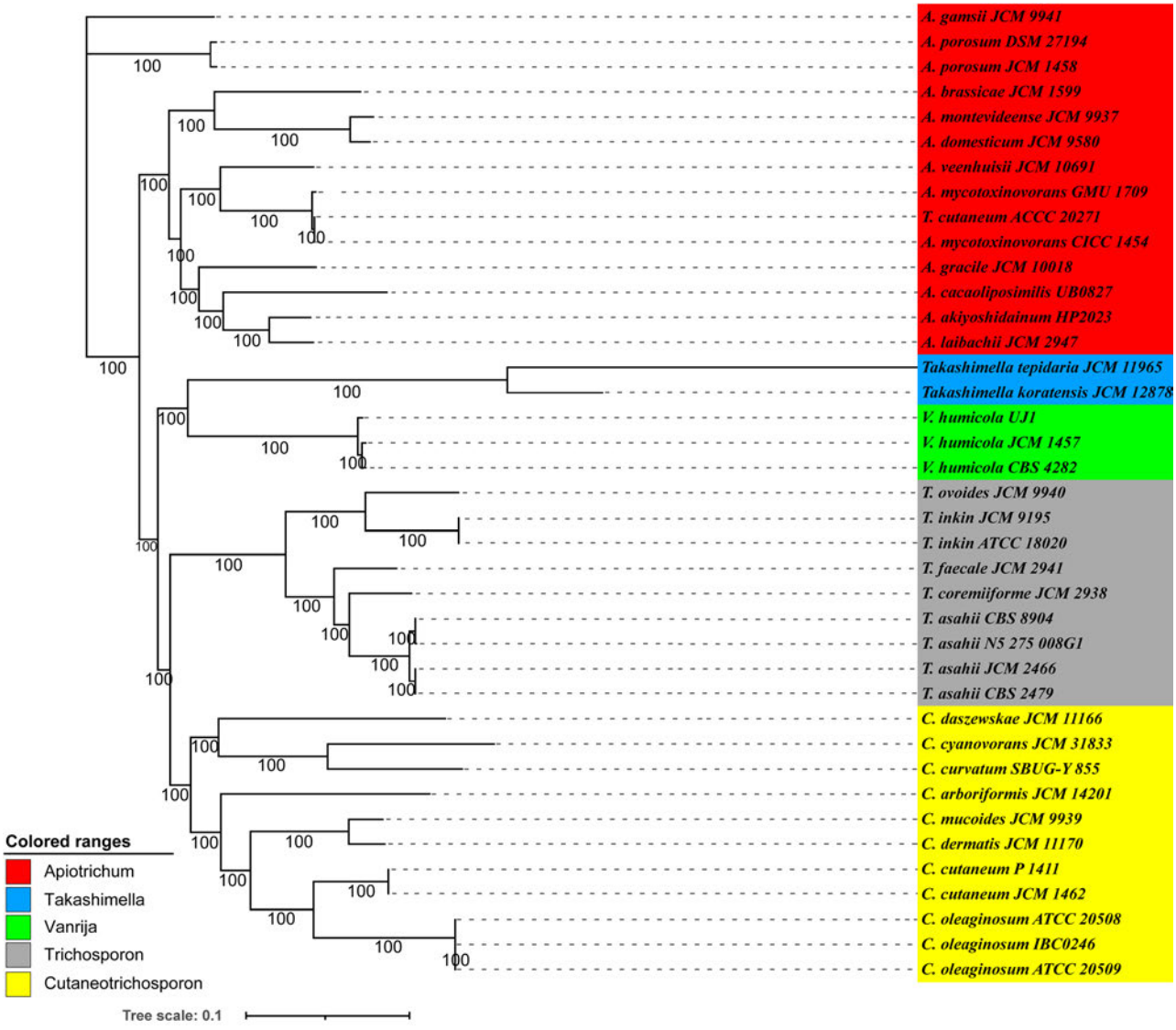

Fig. 3. A phylogenomic analysis of the thirty-seven members of the *Trichosporonaceae* family, conducted using the maximum likelihood (ML) method. The ML tree was constructed based on the concatenated non-gapped sites from multiple whole-genome alignments. The branch length of this tree represented the evolutionary distance on the tree scale. The phylogenetic analysis was conducted using raxmlHPC-PTHREADS-AVX (v8.2.13), utilizing the GTRGAMMA model and 1,000 bootstrap replicates. The genera *Apiotrichum*, *Trichosporon*, *Cutaneotrichosporon*, and *Vanrija* within the *Trichosporonaceae* family and the genus *Takashimella* (outgroup) in *Tetragoniomycetaceae* are highlighted in red, gray, yellow, green, and blue, respectively.

intrinsically to pathogenicity. *A. cacaoliposimilis* is an emerging opportunistic pathogen that exhibits pathogenicity through invasive manipulation and immunodeficiency (Noguchi et al. 2020). A comparison of the PHI databases under the ULTRA SENSITIVE mode of blast search conducted in the present study revealed 741 PHI homologous genes, which was higher than the average in all compared strains (704). Further analysis with the terms "Primates", "Birds", "Rabbits & hares", "Nematodes", "Flies", "Bony fishes", and "Rodents" used under the category of interacting hosts identified 296 PHI homologous genes (6% hypervirulence, 9% lethal, 14% loss of pathogenicity, 18% unaffected pathogenicity, and 51% reduced virulence). These organisms were explicitly selected as they have frequently been utilized in various studies as models to understand human diseases better.

A higher number of PHI genes were detected in the environmental isolate *A. porosum* DSM27194. Grouping of the strains based on their origin (environmental and clinical) and the statistical analysis based on the Wilcoxon rank-sum test revealed non-significant differences ($p > 0.05$). The inter-species comparison of *A. cacaoliposimilis* UB0827 was performed using two grouping methods: one based on *A. cacaoliposimilis* UB0827 and other species and the other based on genera. A comparison of the differences between these two groups identified 215 significant PHI-base accessions (210 intergeneric and five inter-specific differences). Specifically, 72 intergeneric ($p < 0.001$) and

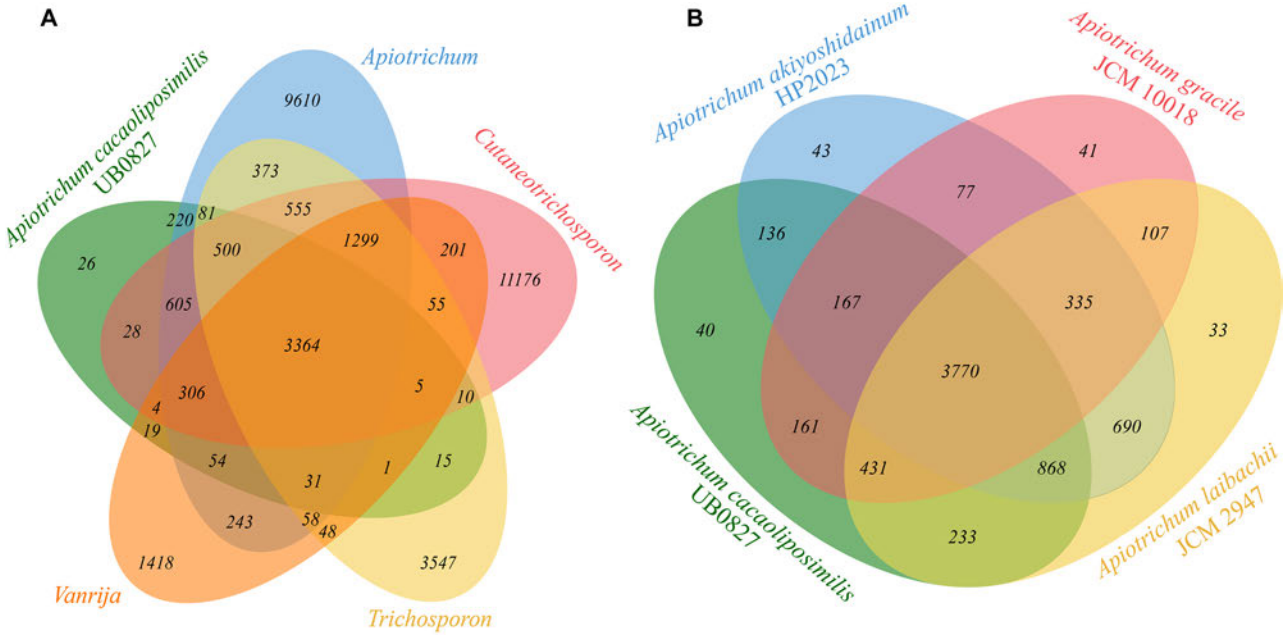

Fig. 4. A) Venn diagram illustrating the relationships between *A. cacaoliposimilis* UB0827 and the different *Trichosporonaceae* genera based on the 6656 orthogroups; B) Venn diagram illustrating the relationships among different species positioned on the same node.

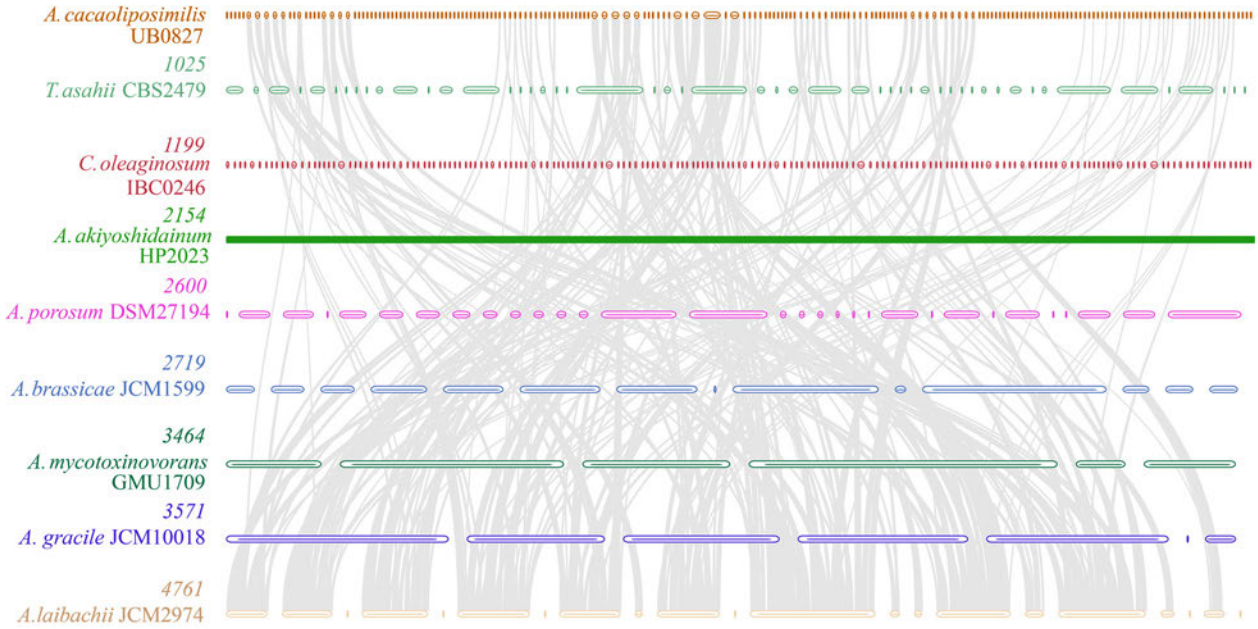

Fig. 5. The synteny analysis performed at the genomic level for strain UB0827 and the representative strains of different nodes. The number displayed between the strains indicates the number of syntenic blocks, which become increasingly dense when moving from top to bottom. The straight line exists due to the poor assembly quality of the HP2023 strain.

five interspecific ($p < 0.05$) differences in PHI were noted (Fig. 6B). The PHI accessions of the inter-specific differences included PHI: 273, PHI: 4878, PHI: 6444, PHI: 6752, and PHI: 8598, which encode the SAGA complex species spt3 protein (*spt3*), a putative serine/threonine protein phosphatase type 2A (*ppg1*), NADH-ubiquinone oxidoreductase 299 kDa subunit (*Complex I NADH oxidoredutase*), F-box Protein Fbx15 (*grrA*), and chitin deacetylase (*cda1*, except for UB0827), respectively. The inter-generic comparisons were conducted by compiling a detailed catalog (Table SII) of all PHI genes in UB0827, including the four inter-species differential genes. While 60% of the causative genes were revealed to be associated with lung tissue, 40% were associated with metabolic enzyme reactions. Among the highly pathogenic genes, PHI: 5267 and PHI: 8896 were specific to the *Apiotrichum* genus and encoded epimerase (*ugeB*) and

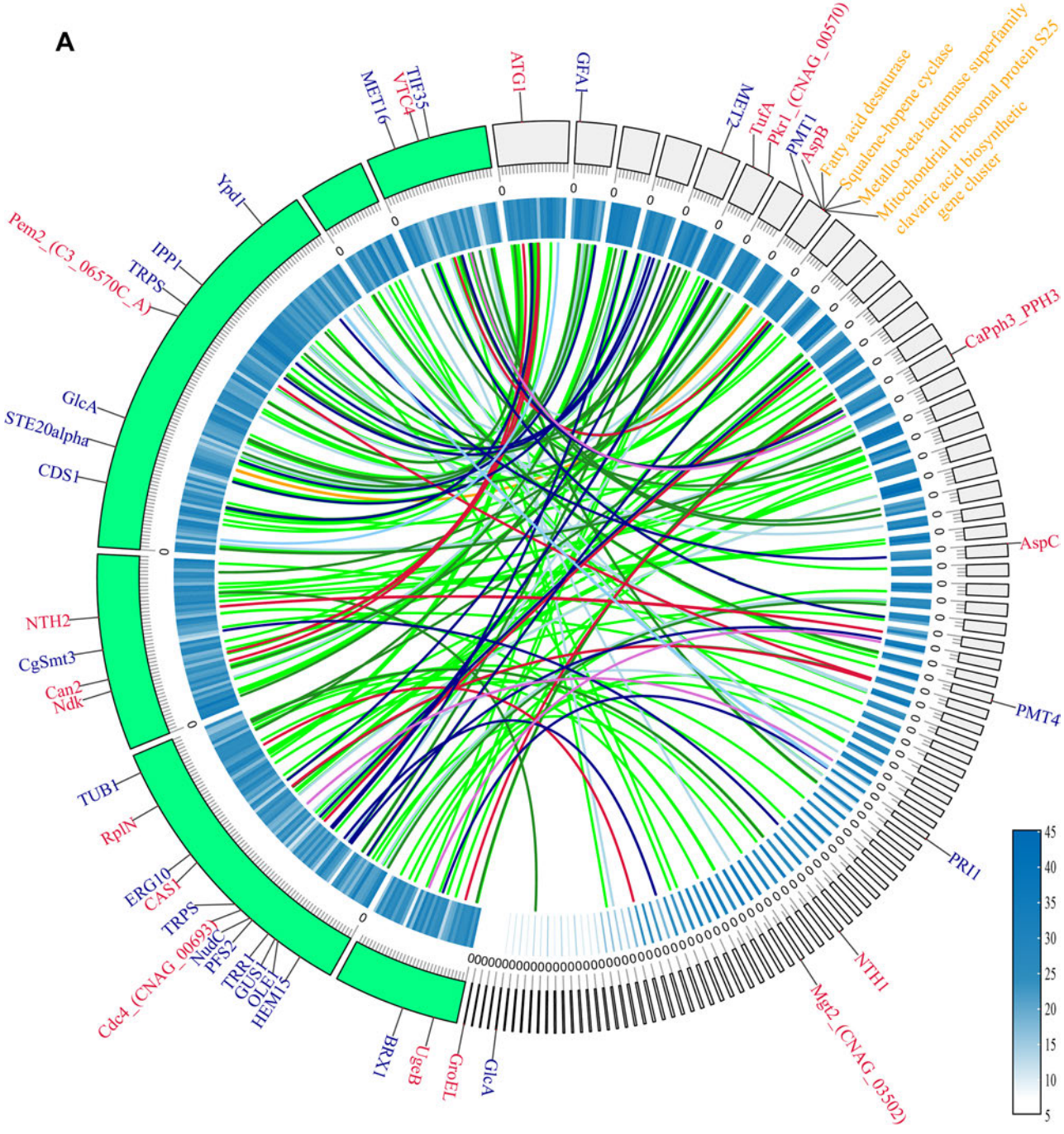

Fig. 6. A) The outermost circle represents the chromosome skeleton, with strain GMU1709 depicted in green and strain UB0827 depicted in light grey. The inner circle indicates gene density, with a gradient from white to blue indicating an increase in the number of genes. Syntenic pairs indicate the shared pathogenic genes. The genes depicted on the left skeleton are shared genes, while the genes depicted on the right skeleton are the genes specific to *A. cacaoliposimilis*. The colors of the genes indicate their respective phenotypic classifications.

phosphatidyl-*N*-methylethanolamine *N*-methyltransferase (*pem2*), respectively. PHI: 9135, which encodes serine/threonine-protein kinase (*atg1*), was more common in the *Cutaneotrichosporon* genus. Moreover, considering the syntenic relationship, 64.86% (192 of 296) of the pathogenic genes were common to the pathogenic strains UB0827 and GMU1709 (Fig. 6A) and included nine genes associated with high virulence and 19 lethal factors. In addition, nine hypervirulence genes (*atg1*, *tufa*, *pkr1*, *aspB*, *CaPph3*, *aspC*, *nth1*, *mgt2*, and *GroEL*) and six lethal factors (*gfa1*, *met2*, *pmt1*, *pmt4*, *pri1*, and *glcA*) were specific to UB0827.

Discussion

The first strain of *A. cacaoliposimilis*, which could produce lipids resembling natural cocoa butter, was isolated from the soil (Gujjari et al. 2011). The fungi of this

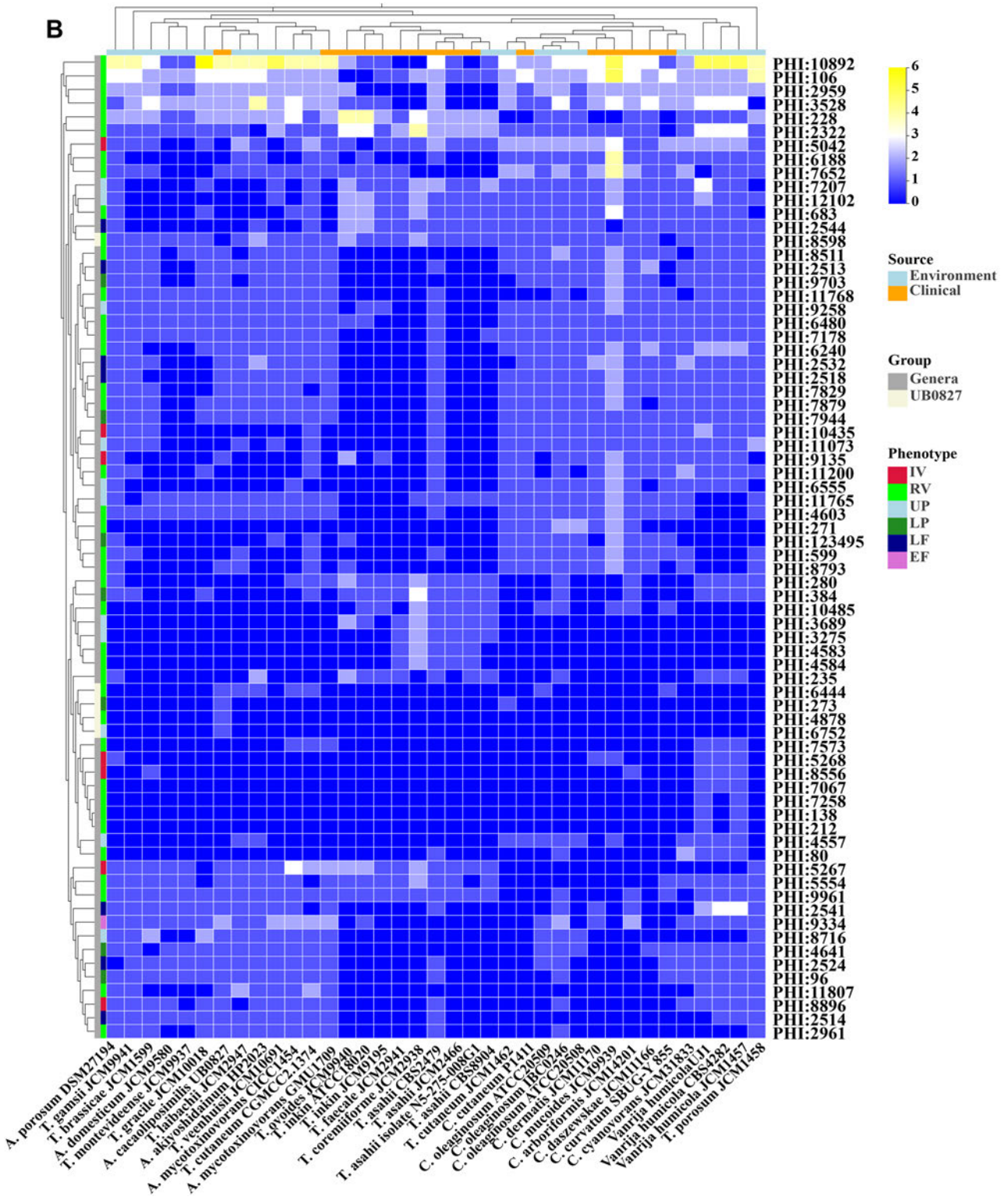

Fig. 6. B) A total of 77 disease-causing genes are depicted, with 72 of these genes differing between the various genera and 5 genes differing between species. The outermost color on the left corresponds to the grouping, while the innermost color represents the phenotypic classification of the disease-causing genes. The top hints at the origin of the isolated strain. The gradient from dark blue to yellow indicates an increase in the number of genes.

species are considered essential producers of biological lipids (Silva et al. 2023) and cocoa butter alternatives (Yang et al. 2024). The predominant method for the clinical detection of *A. cacaoliposimilis* involves culturing for morphological identification, followed by biochemical analyses for species determination. However, a limitation of this approach is that it does not identify and differentiate the closely related species precisely. Considering the distinct pathogenic effects and drug resistance profiles of various fungal species within the

Apiotrichum genus, accurate identification is crucial for the clinical prevention and treatment of infections caused by these fungi. Mass spectrometry and molecular identification have facilitated more access to precise species identification. Mass spectrometry is instrumental in identifying *Trichosporon* genus, although it exhibits lower effectiveness for *Apiotrichum* genus (de Almeida et al. 2017; Ahangarkani et al. 2021). Over the past decade, the focus of molecular identification analyses has shifted from phenotypic to molecular markers. For instance, basidiomycetous fungi may be identified based on the GC molar ratio of their nuclear DNA, which ranges from 50% to 70% (Kurtzman 2006). ITS sequences are invaluable for accurate species identification, as demonstrated previously in studies conducted with yeast microbiota (García-Béjar et al. 2023). In the present study, first-generation sequencing technology was utilized to retrieve the ITS segments of a fungus that closely resembled *A. cacaoliposimilis* ATCC® 20505™ (identities 485/488, gaps 3/488; Fig. S1a) and was different from *A. akiyoshidainum* M8 (formerly known as *Trichosporon akiyoshidainum*, identities 482/485, gaps 2/485). Since the nucleotide sequence differences between *A. cacaoliposimilis* and *A. akiyoshidainum* were revealed to be mostly present in the D1/D2 region (Gujjari et al. 2011), a phylogenetic tree was constructed using the ITS regions. The tree validated that the isolated fungus was closest to *A. akiyoshidainum* or *A. cacaoliposimilis*, although with a lower bootstrap value, possibly due to the shorter sequences and the influence of the conserved loci (Paradis et al. 2023). Differential evolution or horizontal gene transfer may skew the topology of the phylogenetic tree constructed based on limited genes, leading to misrepresentation of the phylogenetic relationships. Therefore, a genome-wide phylogenetic analysis was conducted in the present study. Multiple sequence comparisons among the significant genera within *Trichosporonaceae* confirmed that the isolated fungus was *A. cacaoliposimilis*. Genome homologous family analysis and genome synteny analysis also corroborated this finding.

Biochemical analyses are often used as a crucial tool in fungal identification. However, these analyses are not commonly used as routine clinical tests due to their low accuracy and limited clinical benefit. In the present study, the biochemical reactions of the clinical isolates *A. cacaoliposimilis* UB0827 and *A. mycotoxinivorans* GMU 1709 (Peng et al. 2019) were compared with those of the environmental isolate *A. cacaoliposimilis* ATCC® 20505™ (Gujjari et al. 2011). The differential results obtained are presented in Table I. Certain assimilations, including glycerol, D-melibiose, D-melezitose, and sorbose assimilation, were weaker in the two clinical isolates than those in the environmental isolated strain ATCC® 20505™. These observations, together with the annotations from the CAZy database, revealed that the UB0827 strain had non-significantly higher levels of glycosyltransferases than those noted in GMU1709.

Further, the clinical isolates did not produce β-*N*-acetylglucosaminidase, while the environmental isolate was positive in the D-glucosamine reaction test. Both the clinical and environmental isolates exhibited a rough phenotype. These findings contrast with those reported by Ichikawa et al. (2004), suggesting that the selective evolution has been possibly influenced by the absence of glucose in the urine. Consistent with characteristics typical of the *Trichosporon* genus, *A. cacaoliposimilis* produces urease (Ashok et al. 2019), which is a distinguishing feature for identifying the fungi belonging to this group.

Clinical research on the species related closely to the *Trichosporon* genus has revealed that these fungi are opportunistic pathogens, particularly in patients admitted to the intensive care units and undergoing invasive procedures and treatment with broad-spectrum antibiotics (Ahangarkani et al. 2021). This represents a significant challenge for the future applications of food additives. Epidemiological studies conducted in Brazil and China have indicated a predominance of infections caused by *T. asahii* cultured from the samples collected from the urinary tract (de Almeida et al. 2017; Francisco et al. 2019). Since the *Apiotrichum* genus reclassified in 2015 (Liu et al. 2015b), its clinical pathogenicity has been increasingly recognized. Lara et al. (2019) isolated *Apiotrichum veenhuisii* from the skin of pediatric patients with acute myeloid leukemia. Peng et al. (2019) reported the presence of *A. mycotoxinovorans* in the sputum of a pediatric patient with congenital heart disease and pneumonia. Noguchi et al. (2020) isolated *A. cacaoliposimilis* from the fingernails of a geriatric patient with interstitial pneumonia. These findings indicate the pathogenic potential of the *Apiotrichum* genus. In the present study, *A. cacaoliposimilis* UB0827 was isolated from the clear mid-stream urine of a patient with UTI who had undergone invasive catheterization and exhibited improvement after antifungal treatment. The present study revealed intergeneric variations in the epimerase gene (PHI: 5267), which is involved in the synthesis of galactosaminogalactan, a substance capable of modulating host immune response and enhancing pathogenicity (Lee et al. 2015).

Similarly, the gene encoding phosphatidyl-*N*-(methylethanolamine) *N*-methyltransferase (PHI: 8896), which is involved in the CDP-DAG pathway, was revealed to be functional in UB0827 (Tams et al. 2019). The CDP-DAG pathway is significant for synthesizing critical phosphatidic acids, such as phosphatidylserine, phosphatidylethanolamine, and phosphatidylcholine in *Candida albicans*. These phospholipids are essential components of the fungal cell membrane and play criti-

cal roles in maintaining cell structure, signaling, and membrane trafficking. The gene encoding serine/threonine-protein kinase (PHI: 9135) is primarily involved in the formation and degradation of autophagosomes, particularly those in the kidney (Ding et al. 2018).

Further, the present study identified *cdc4* (PHI: 11985), which encodes a member of the F-box protein family, in the isolated fungus. This gene plays a crucial role in several biological processes, including the cell cycle and fungal infectivity, as the protein encoded by this gene recognizes and ubiquitinates substrates via the ubiquitin ligase E3 complex (Wu et al. 2022). In the pathogenicity syntenic analysis of the clinical strain GMU1709, several independent pathogenicity genes were identified initially, although a few of these genes had to be excluded due to the stringent comparison model. Ultimately, only the high virulence genes *aspB* and *aspC*, and the lethal factors *pmt4*, *pri1*, *met2*, and *pmt1* that belonged to UB0827 alone, were retained. The genes *aspB* and *aspC*, mainly are involved in synthesizing septins, a group of GTPases crucial for maintaining the integrity of the fungal cell wall. The absence of septins could compromise the invasive capabilities of a fungus (Vargas-Muñiz et al. 2015). These findings suggested a direct link between the identified causative genes and the opportunistic infections caused by *A. cacaoliposimilis*. However, since this strain is the first to be identified and has its whole-genome sequencing data unavailable, intraspecies comparisons could not be conducted at present, and classification based on the clinical origin of the strain did not yield significant results.

The *in vitro* drug sensitivity assessments revealed that *A. cacaoliposimilis* was particularly susceptible to triazole antifungal medications, demonstrating the highest sensitivity to voriconazole and posaconazole. Itraconazole was also effective against *A. cacaoliposimilis*, while fluconazole exhibited a relatively lower activity against this fungus. These findings are consistent with the drug sensitivity statistics reported for the *Trichosporon* genus in recent years (Francisco et al. 2019; Ahangarkani et al. 2021). However, *A. mycotoxinovorans* GMU 1709 exhibited less sensitivity to voriconazole compared to itraconazole (Peng et al. 2019), and the literature contains reports of the latter being used prophylactically for *T. asahii* infections (Asada et al. 2006). In contrast to *A. mycotoxinovorans*, *A. cacaoliposimilis* exhibited sensitivity to 5-fluorocytosine. Amphotericin-B was highly effective against *A. cacaoliposimilis*, while anidulafungin and micafungin exhibited reduced activity, consistent with the previous reports on *A. veenhuisii* (Lara et al. 2019). Moreover, a comparison with the Comprehensive Antibiotic Resistance Database revealed abundant primary resistance mechanisms, such as efflux, reduced antibiotic permeability, and target alteration-related proteins, in UB0827. These mechanisms are the primary factors underlying echinocandin resistance in the related *Apiotrichum* spp. (Franconi and Lupetti 2023). When selecting antifungal agents for patients with renal impairments or those at risk of this condition, it is important to consider the pharmacokinetic properties and nephrotoxic potential of such agents to ensure the safety and effectiveness of prophylaxis or treatment (Tragiannidis et al. 2021). Therefore, empirical antifungal therapy alone is inadequate, and routine drug susceptibility testing is necessary.

In summary, infections with *Apiotrichum* spp. are relatively rare and reported primarily in cutaneous infections. The urinary tract infections (UTIs) involving this genus are usually associated with invasive procedures such as catheterization, which may facilitate fungal colonization. The present study pioneers in reporting the case of an *A. cacaoliposimilis* strain isolated from the urine sample of a patient with UTI. The present study's findings are valuable for understanding the clinical characteristics of this fungus. Triazole antibiotics are used empirically for the treatment of *A. cacaoliposimilis* infections. The subsequent genome-wide analysis classified *A. cacaoliposimilis* within the *Trichosporonaceae* family. Identifying distinct inter-generic virulence genes supported the independent positioning of the *Apiotrichum* genus from the *Trichosporon* genus in the evolutionary setup. In addition to underscoring the taxonomic separation, the differentiation provides insights for future research on the possible pathogenic mechanisms of these genera.

Availability of data and material

Data from this study will be fully available and without restriction upon reasonable request. The ITS sequence and WGS data will upload PRJNA1062540 on NCBI. This Whole Genome Shotgun project has been deposited at DDBJ/ENA/GenBank under the accession GCA_040285315.1.

Ethical statement

The study was approved by the Ethics Committee of the First Affiliated Hospital of Nanchang University (Nanchang, China [approval number: 2014036]). All patients had informed consent for study participation, and all personal data were kept confidential. At the same time, we confirmed that the relevant guidelines and regulations in China used all the methods.

Author contributions

K.S.C. and W.W. contributed to study design, data analysis, and manuscript writing. W.W., J.P.Y., J.H.Z., D.L, Q.C., S.M.Y., and L.X. participated in study design, data collection, and analysis. W.W., J.H.Z., S.M.Y., and L.Y. conducted laboratory testing. W.W. and K.S.C. revised and polished the manuscript. All the authors have read the final version of the manuscript and have approved it.

Funding

This work was supported by the National Natural Science Foundation of China (NO. 82060611) and Jiangxi Provincial Department of Science and Technology (NO. 20212BDH81017). The funder had no role in study design, data collection and analysis, decision to publish, or preparation of the manuscript.

Conflict of interest

The authors do not report any financial or personal connections with other persons or organizations, which might negatively affect the contents of this publication and/or claim authorship rights to this publication.

Literature

Ahangarkani F, Ilkit M, Vaseghi N, Zahedi N, Zomorodian K, Khodavaisy S, Afsarian MH, Abbasi K, de Groot T, Meis JF, et al. MALDI-TOF MS characterisation, genetic diversity and antifungal susceptibility of *Trichosporon* species from Iranian clinical samples. Mycoses. 2021 Aug;64(8):918–925. https://doi.org/10.1111/myc.13306

Alcock BP, Huynh W, Chalil R, Smith KW, Raphenya AR, Wlodarski MA, Edalatmand A, Petkau A, Syed SA, Tsang KK, et al. CARD 2023: Expanded curation, support for machine learning, and resistome prediction at the Comprehensive Antibiotic Resistance Database. Nucleic Acids Res. 2023 Jan;51(D1):D690–D699. https://doi.org/10.1093/nar/gkac920

Angiuoli SV, Salzberg SL. Mugsy: Fast multiple alignment of closely related whole genomes. Bioinformatics. 2011 Feb;27(3):334–42. https://doi.org/10.1093/bioinformatics/btq665

Asada N, Uryu H, Koseki M, Takeuchi M, Komatsu M, Matsue K. Successful treatment of breakthrough *Trichosporon asahii* fungemia with voriconazole in a patient with acute myeloid leukemia. Clin Infect Dis. 2006 Aug;43(4):e39–e41. https://doi.org/10.1086/505970

Ashok A, Doriya K, Rao JV, Qureshi A, Tiwari AK, Kumar DS. Microbes producing L-asparaginase free of glutaminase and urease isolated from extreme locations of Antarctic soil and moss. Sci Rep. 2019 Feb;9(1):1423. https://doi.org/10.1038/s41598-018-38094-1

Benson G. Tandem repeats finder: A program to analyze DNA sequences. Nucleic Acids Res. 1999 Jan 15;27(2):573–580. https://doi.org/10.1093/nar/27.2.573

Blin K, Medema MH, Kazempour D, Fischbach MA, Breitling R, Takano E, Weber T. antiSMASH 2.0 – A versatile platform for genome mining of secondary metabolite producers. Nucleic Acids Res. 2013 Jul;41(W1):W204–W212. https://doi.org/10.1093/nar/gkt449

Buchfink B, Reuter K, Drost HG. Sensitive protein alignments at tree-of-life scale using DIAMOND. Nat Methods. 2021 Apr; 18(4):366–368. https://doi.org/10.1038/s41592-021-01101-x

Capella-Gutiérrez S, Silla-Martínez JM, Gabaldón T. trimAl: A tool for automated alignment trimming in large-scale phylogenetic analyses. Bioinformatics. 2009 Aug ;25(15):1972–1973. https://doi.org/10.1093/bioinformatics/btp348

Chen C, Wu Y, Li J, Wang X, Zeng Z, Xu J, Liu Y, Feng J, Chen H, He Y, et al. TBtools-II: A "one for all, all for one" bioinformatics platform for biological big-data mining. Mol Plant. 2023 Nov;16(11): 1733–1742. https://doi.org/10.1016/j.molp.2023.09.010

Colombo AL, Padovan AC, Chaves GM. Current knowledge of *Trichosporon* spp. and trichosporonosis. Clin Microbiol Rev. 2011 Oct;24(4):682–700. https://doi.org/10.1128/cmr.00003-11

de Almeida JN Jr, Favero Gimenes VM, Francisco EC, Machado Siqueira LP, Gonçalves de Almeida RK, Guitard J, Hennequin C, Colombo AL, Benard G, Rossi F. Evaluating and improving Vitek MS for identification of clinically relevant species of *Trichosporon* and the closely related genera *Cutaneotrichosporon* and *Apiotrichum*. J Clin Microbiol. 2017 Aug;55(8):2439–2444. https://doi.org/10.1128/JCM.00461-17

Ding H, Caza M, Dong Y, Arif AA, Horianopoulos LC, Hu G, Johnson P, Kronstad JW. *ATG* genes influence the virulence of *Cryptococcus neoformans* through contributions beyond core autophagy functions. Infect Immun. 2018 Aug;86(9):e00069-18. https://doi.org/10.1128/iai.00069-18

Edgar RC. Muscle5: High-accuracy alignment ensembles enable unbiased assessments of sequence homology and phylogeny. Nat Commun. 2022 Nov;13(1):6968. https://doi.org/10.1038/s41467-022-34630-w

Francisco EC, de Almeida Junior JN, de Queiroz Telles F, Aquino VR, Mendes AVA, de Andrade Barberino MGM, de Tarso O Castro P, Guimarães T, Hahn RC, Padovan ACB, et al. Species distribution and antifungal susceptibility of 358 *Trichosporon* clinical isolates collected in 24 medical centres. Clin Microbiol Infect. 2019 Jul; 25(7):909.e1–909.e5. https://doi.org/10.1016/j.cmi.2019.03.026

Francisco EC, Ebbing M, Colombo AL, Hagen F; Trichosporon Brazilian Network. Identification of clinical *Trichosporon asteroides* strains by MALDI-TOF Mass Spectrometry: Evaluation of the Bruker Daltonics Commercial System and an in-house developed library. Mycopathologia. 2023 Jun;188(3):243–249. https://doi.org/10.1007/s11046-023-00723-3

Franconi I, Lupetti A. In Vitro susceptibility tests in the context of antifungal resistance: Beyond minimum inhibitory concentration in *Candida* spp. J Fungi. 2023 Dec;9(12):1188. https://doi.org/10.3390/jof9121188

Galaxy Community. The Galaxy platform for accessible, reproducible and collaborative biomedical analyses: 2022 update. Nucleic Acids Res. 2022 Jul;50(W1):W345–W351. https://doi.org/10.1093/nar/gkac247

García-Béjar B, Fernández-Pacheco P, Carreño-Domínguez J, Briones A, Arévalo-Villena M. Identification and biotechnological characterisation of yeast microbiota involved in spontaneous fermented wholegrain sourdoughs. J Sci Food Agric. 2023 Dec; 103(15):7683–7693. https://doi.org/10.1002/jsfa.12864

Ghazani SM, Marangoni AG. Microbial lipids for foods. Trends Food Sci Technol. 2022 Jan;119:593–607. https://doi.org/10.1016/j.tifs.2021.10.014

Gujjari P, Suh SO, Coumes K, Zhou JJ. Characterization of oleaginous yeasts revealed two novel species: *Trichosporon cacaoliposimilis* sp. nov. and *Trichosporon oleaginosus* sp. nov. Mycologia. 2011 Sep-Oct;103(5): 1110–1118. https://doi.org/10.3852/10-403

Guo LN, Xiao M, Kong F, Chen SC, Wang H, Sorrell TC, Jiang W, Dou HT, Li RY, Xu YC. Three-locus identification, genotyping, and antifungal susceptibilities of medically important *Trichosporon* species from China. J Clin Microbiol. 2011 Nov;49(11):3805–3811. https://doi.org/10.1128/jcm.00937-11

Guo LN, Yu SY, Hsueh PR, Al-Hatmi AMS, Meis JF, Hagen F, Xiao M, Wang H, Barresi C, Zhou ML, et al. Invasive infections due to *Trichosporon*: species distribution, genotyping, and antifungal susceptibilities from a multicenter study in China. J Clin Microbiol. 2019 Jan;57(2):e01505–18. https://doi.org/10.1128/jcm.01505-18

Ichikawa T, Sugita T, Wang L, Yokoyama K, Nishimura K, Nishikawa A. Phenotypic switching and beta-*N*-acetylhexosaminidase activity of the pathogenic yeast *Trichosporon asahii*. Microbiol Immunol. 2004;48(4):237–242. https://doi.org/10.1111/j.1348-0421.2004.tb03519.x

Kalvari I, Nawrocki EP, Ontiveros-Palacios N, Argasinska J, Lamkiewicz K, Marz M, Griffiths-Jones S, Toffano-Nioche C, Gautheret D, Weinberg Z, et al. Rfam 14: Expanded coverage of metagenomic, viral and microRNA families. Nucleic Acids Res. 2021 Jan;49(D1):D192–D200. https://doi.org/10.1093/nar/gkaa1047

Kim JS, Seo SG, Jun BK, Kim JW, Kim SH. Simple and reliable DNA extraction method for the dark pigmented fungus, *Cercospora sojina*. Plant Pathol J. 2010;26(3):289–292. https://doi.org/10.5423/ppj.2010.26.3.289

Krogh A, Larsson B, von Heijne G, Sonnhammer EL. Predicting transmembrane protein topology with a hidden Markov model: Application to complete genomes. J Mol Biol. 2001 Jan;305(3):567–580. https://doi.org/10.1006/jmbi.2000.4315

Kurtzman CP. Yeast species recognition from gene sequence analyses and other molecular methods. Mycoscience. 2006 Apr;47(2):65–71. https://doi.org/10.1007/s10267-006-0280-1

Lagesen K, Hallin P, Rødland EA, Staerfeldt HH, Rognes T, Ussery DW. RNAmmer: Consistent and rapid annotation of ribosomal RNA genes. Nucleic Acids Res. 2007;35(9):3100–3108. https://doi.org/10.1093/nar/gkm160

Langsiri N, Worasilchai N, Irinyi L, Jenjaroenpun P, Wongsurawat T, Luangsa-Ard JJ, Meyer W, Chindamporn A. Targeted sequencing analysis pipeline for species identification of human pathogenic fungi using long-read nanopore sequencing. IMA Fungus. 2023 Sep;14(1):18. https://doi.org/10.1186/s43008-023-00125-6

Lara BR, Melo MBA, Paula CR, Arnoni MV, Simões CCN, Nakano S, Richini-Pereira VB, Garces HG, Maciel da Silva BC, Anversa L, et al. *Apiotrichum veenhuisii* isolated from a pediatric patient with acute myeloid leukemia: The first case in humans. Mycologia. 2019 Sep-Oct;111(5):793–797. https://doi.org/10.1080/00275514.2019.1637645

Lee MJ, Liu H, Barker BM, Snarr BD, Gravelat FN, Al Abdallah Q, Gavino C, Baistrocchi SR, Ostapska H, Xiao T, et al. The fungal exopolysaccharide galactosaminogalactan mediates virulence by enhancing resistance to neutrophil extracellular traps. PLoS Pathog. 2015 Oct;11(10):e1005187. https://doi.org/10.1371/journal.ppat.1005187

Liu XZ, Wang QM, Göker M, Groenewald M, Kachalkin AV, Lumbsch HT, Millanes AM, Wedin M, Yurkov AM, Boekhout T, et al. Towards an integrated phylogenetic classification of the *Tremellomycetes*. Stud Mycol. 2015a Jun;81:85–147. https://doi.org/10.1016/j.simyco.2015.12.001

Liu XZ, Wang QM, Theelen B, Groenewald M, Bai FY, Boekhout T. Phylogeny of tremellomycetous yeasts and related dimorphic and filamentous basidiomycetes reconstructed from multiple gene sequence analyses. Stud Mycol. 2015b Jun;81:1–26. https://doi.org/10.1016/j.simyco.2015.08.001

Lowe TM, Eddy SR. tRNAscan-SE: A program for improved detection of transfer RNA genes in genomic sequence. Nucleic Acids Res. 1997 Mar;25(5):955–964. https://doi.org/10.1093/nar/25.5.955

Luo R, Liu B, Xie Y, Li Z, Huang W, Yuan J, He G, Chen Y, Pan Q, Liu Y, et al. SOAPdenovo2: An empirically improved memory-efficient short-read de novo assembler. Gigascience. 2012 Dec;1(1):18. https://doi.org/10.1186/2047-217X-1-18

Minh BQ, Schmidt HA, Chernomor O, Schrempf D, Woodhams MD, von Haeseler A, Lanfear R. IQ-TREE 2: New models and efficient methods for phylogenetic inference in the genomic era. Mol Biol Evol. 2020 May;37(5):1530–1534. https://doi.org/10.1093/molbev/msaa015

Nash A, Sewell T, Farrer RA, Abdolrasouli A, Shelton JMG, Fisher MC, Rhodes J. MARDy: Mycology Antifungal Resistance Database. Bioinformatics. 2018 Sep;34(18):3233–3234. https://doi.org/10.1093/bioinformatics/bty321

Noguchi H, Matsumoto T, Kimura U, Hiruma M, Kano R, Yaguchi T, Fukushima S, Ihn H. Onychomycosis caused by *Trichosporon cacaoliposimilis*. J Dermatol. 2020 May;47(5):e193–e195. https://doi.org/10.1111/1346-8138.15305

Palmer JM, Stajich J. Funannotate v1.8.1: Eukaryotic genome annotation. Zenodo. 2020. https://doi.org/10.5281/zenodo.4054262

Paradis E, Claramunt S, Brown J, Schliep K. Confidence intervals in molecular dating by maximum likelihood. Mol Phylogenet Evol. 2023 Jan;178:107652. https://doi.org/10.1016/j.ympev.2022.107652

Peng L, Jiang YQ, Jiang GM, Ou JY, Zeng LT, Zhang HH, Chen DQ, Jiang YT. Molecular identification and biological characteristic analysis of an *Apiotrichum mycotoxinivorans* (formerly *Trichosporon mycotoxinivorans*) strain isolated from sputum specimens of a pediatric patient with pneumonia. J Mycol Med. 2019 Jun;29(2):120–126. https://doi.org/10.1016/j.mycmed.2019.01.010

Peng L, Liu CF, Wu H, Jin H, Deng XY, Zeng LT, Xiao Y, Deng C, Yang ZK. Complete genome sequencing and comparative analysis of the clinically-derived *Apiotrichum mycotoxinivorans* strain GMU1709. Front Cell Infect Microbiol. 2022 Feb;12:834015. https://doi.org/10.3389/fcimb.2022.834015

Petersen TN, Brunak S, von Heijne G, Nielsen H. SignalP 4.0: Discriminating signal peptides from transmembrane regions. Nat Methods. 2011 Sep;8(10):785–786. https://doi.org/10.1038/nmeth.1701

Premamalini T, Anitha S, Rajyoganandh SV, Veena H, Kindo AJ. Complicated urinary tract infection by *Trichosporon loubieri*. Med Mycol Case Rep. 2019 Apr;24:86–89. https://doi.org/10.1016/j.mmcr.2019.04.014

Rozewicki J, Li S, Amada KM, Standley DM, Katoh K. MAFFT-DASH: Integrated protein sequence and structural alignment. Nucleic Acids Res. 2019 Jul;47(W1):W5–W10. https://doi.org/10.1093/nar/gkz342

Shen W, Le S, Li Y, Hu F. SeqKit: A cross-platform and ultrafast toolkit for FASTA/Q file manipulation. PLoS One. 2016 Oct; 11(10): e0163962. https://doi.org/10.1371/journal.pone.0163962

Shen W, Sipos B, Zhao L. SeqKit2: A Swiss army knife for sequence and alignment processing. Imeta. 2024 Apr;3(3):e191. https://doi.org/10.1002/imt2.191

Silva JME, Martins LHDS, Moreira DKT, Silva LDP, Barbosa PPM, Komesu A, Ferreira NR, Oliveira JAR. Microbial lipid based biorefinery concepts: A review of status and prospects. Foods. 2023 May; 12(10):2074. https://doi.org/10.3390/foods12102074

Simão FA, Waterhouse RM, Ioannidis P, Kriventseva EV, Zdobnov EM. BUSCO: Assessing genome assembly and annotation completeness with single-copy orthologs. Bioinformatics. 2015 Oct; 31(19):3210–3212. https://doi.org/10.1093/bioinformatics/btv351

Sonnhammer EL, von Heijne G, Krogh A. A hidden Markov model for predicting transmembrane helices in protein sequences. Proc Int Conf Intell Syst Mol Biol. 1998;6:175–182.

Stamatakis A. RAxML version 8: A tool for phylogenetic analysis and post-analysis of large phylogenies. Bioinformatics. 2014 May; 30(9):1312–1313. https://doi.org/10.1093/bioinformatics/btu033

Tams RN, Cassilly CD, Anaokar S, Brewer WT, Dinsmore JT, Chen YL, Patton-Vogt J, Reynolds TB. Overproduction of phospholipids by the Kennedy pathway leads to hypervirulence in *Candida albicans*. Front Microbiol. 2019 Feb;10:86. https://doi.org/10.3389/fmicb.2019.00086

Taverna CG, Córdoba S, Murisengo OA, Vivot W, Davel G, Bosco-Borgeat ME. Molecular identification, genotyping, and antifungal susceptibility testing of clinically relevant *Trichosporon* species from Argentina. Med Mycol. 2014 May;52(4):356–366. https://doi.org/10.1093/mmy/myt029

Tragiannidis A, Gkampeta A, Vousvouki M, Vasileiou E, Groll AH. Antifungal agents and the kidney: Pharmacokinetics, clinical nephrotoxicity, and interactions. Expert Opin Drug Saf. 2021 Sep; 20(9):1061–1074. https://doi.org/10.1080/14740338.2021.1922667

Urban M, Cuzick A, Seager J, Wood V, Rutherford K, Venkatesh SY, Sahu J, Iyer SV, Khamari L, De Silva N, et al. PHI-base in 2022: A multi-species phenotype database for Pathogen-Host Interactions. Nucleic Acids Res. 2022 Jan;50(D1):D837–D847. https://doi.org/10.1093/nar/gkab1037

Vargas-Muñiz JM, Renshaw H, Richards AD, Lamoth F, Soderblom EJ, Moseley MA, Juvvadi PR, Steinbach WJ. The *Aspergillus fumigatus* septins play pleiotropic roles in septation, conidiation, and cell wall stress, but are dispensable for virulence. Fungal Genet Biol. 2015 Aug;81:41–51. https://doi.org/10.1016/j.fgb.2015.05.014

Wu T, Fan CL, Han LT, Guo YB, Liu TB. Role of F-box protein Cdc4 in fungal virulence and sexual reproduction of *Cryptococcus neoformans*. Front Cell Infect Microbiol. 2022 Jan;11:806465. https://doi.org/10.3389/fcimb.2021.806465

Yang H, Yue K, Bi Y, Zhang L, Chen X, Bi Y. [Advances in the preparation of cocoa butter equivalents] (in Chinese). China Oils Fats. 2024;(04):52–58. https://doi.org/10.19902/j.cnki.zgyz.1003-7969.230257

Supplementary materials are available on the journal's website.